SLO3 auxiliary subunit LRRC52 controls gating of sperm KSPER currents and is critical for normal fertility

Xu-Hui Zeng[a], Chengtao Yang[b], Xiao-Ming Xia[b], Min Liu[a], and Christopher J. Lingle[b,1]

[a]Institute of Life Science, Nanchang University, Nanchang, Jiangxi, China; and [b]Department of Anesthesiology, Washington University School of Medicine, St. Louis, MO 63110

Edited by David E. Clapham, Howard Hughes Medical Institute, Boston Children's Hospital, Boston, MA, and approved January 21, 2015 (received for review December 12, 2014)

Following entry into the female reproductive tract, mammalian sperm undergo a maturation process termed capacitation that results in competence to fertilize ova. Associated with capacitation is an increase in membrane conductance to both Ca^{2+} and K^+, leading to an elevation in cytosolic Ca^{2+} critical for activation of hyperactivated swimming motility. In mice, the Ca^{2+} conductance (alkalization-activated Ca^{2+}-permeable sperm channel, CATSPER) arises from an ensemble of CATSPER subunits, whereas the K^+ conductance (sperm pH-regulated K^+ current, KSPER) arises from a pore-forming ion channel subunit encoded by the *slo3* gene (SLO3) subunit. In the mouse, both CATSPER and KSPER are activated by cytosolic alkalization and a concerted activation of CATSPER and KSPER is likely a common facet of capacitation-associated increases in Ca^{2+} and K^+ conductance among various mammalian species. The properties of heterologously expressed mouse SLO3 channels differ from native mouse KSPER current. Recently, a potential KSPER auxiliary subunit, leucine-rich-repeat-containing protein 52 (LRRC52), was identified in mouse sperm and shown to shift gating of SLO3 to be more equivalent to native KSPER. Here, we show that genetic KO of LRRC52 results in mice with severely impaired fertility. Activation of KSPER current in sperm lacking LRRC52 requires more positive voltages and higher pH than for WT KSPER. These results establish a critical role of LRRC52 in KSPER channels and demonstrate that loss of a non-pore-forming auxiliary subunit results in severe fertility impairment. Furthermore, through analysis of several genotypes that influence KSPER current properties we show that in vitro fertilization competence correlates with the net KSPER conductance available for activation under physiological conditions.

sperm fertility | KSPER | SLO3 channels | auxiliary subunits

Upon entry into the female reproductive tract, mammalian sperm undergo a sequence of maturational steps, collectively termed capacitation, to become competent to fertilize an egg (1, 2). Two important components of this process, thought to be shared among mammalian species, are cytosolic alkalization (3–5) and then an associated increase in cytosolic Ca^{2+} (6, 7). These events are coupled with changes in ionic fluxes in sperm membrane. Over the past 10 y, the application of patch-clamp recording to individual sperm (8) has allowed identification of ionic currents that respond to alkalization and/or Ca^{2+} (9–12). In mouse sperm, alkalization leads to activation of two sperm-specific channels, the Ca^{2+}-permeable CATSPER channel (8–10, 13) and the K^+-permeable KSPER K^+ channel (14, 15). KSPER and CATSPER currents are also present in human sperm (16–18), although intriguingly there seem to be differences in regulation of each channel type between mice and humans (11, 12, 17).

Despite the species-specific differences in the details of their regulation, KSPER and CATSPER are of central importance in sperm function and fertility in both humans and mice. In mouse sperm, KSPER and CATSPER together account for all patch-clamp measurable cation current activated by voltage and alkalization (19) and are thought to act in concert to mediate the changes in membrane cation conductance and Ca^{2+} influx that occur during the onset of capacitation (14, 20). The critical role of both KSPER and CATSPER in the mouse has been established by demonstration that genetic KO of the pore-forming subunits of each channel [KSPER (15, 21) and CATSPER (22–26)] results in infertility and the CATSPER auxiliary δ subunit is also required for fertility (27).

For mouse KSPER, the pore-forming subunit is termed SLO3, encoded by the *kcnu1* (*slo3*) gene (28). SLO3, which is exclusively expressed in testis (15, 28), is a homolog of the Ca^{2+}- and voltage-activated, large-conductance (BK)-type K^+ channel (29) and heterologously expressed SLO3 results in voltage- and alkalization-activated K^+ currents (28). However, heterologously expressed mouse SLO3 channels differ from mouse KSPER current in important ways. Specifically, whereas pH 7 substantially activates KSPER in mouse sperm at membrane potentials (V_m) between −10 and −50 mV, activation of SLO3 channels at pH 7 is scarcely observed even at an activation potential of +100 mV (30, 31). This discrepancy raised the possibility that an additional regulatory partner of SLO3 may be present in mouse sperm. Guided by the discovery of a new type of auxiliary subunit of the BK channel (32), we recently showed that a related subunit, LRRC52 (leucine-rich-repeat-containing protein 52) is selectively expressed in sperm (33). When LRRC52 is coexpressed with SLO3, the gating range of the resulting channels at a given pH is more like that of KSPER in mouse sperm. LRRC52 protein has also been shown to be present in human sperm and, when coexpressed with human SLO3, LRRC52 results in currents with properties similar to

Significance

Mammalian sperm fertility depends on coordinated activation of two sperm-specific ion channels, the alkalization-activated Ca^{2+}-permeable sperm channel and a sperm pH-regulated K^+ current (KSPER) channel; both are required for fertility. In the mouse, the KSPER channel is thought to involve a complex of a pore-forming ion channel protein and subunit encoded by the *slo3* gene subunit and the leucine-rich-repeat-containing protein 52 (LRRC52) auxiliary subunit. We now show that KO of LRRC52 results in severely compromised fertility and shifts KSPER current activation away from the physiological range. Furthermore, utilizing genotypes with differing average amounts of KSPER current, we show that sperm fertility exhibits a steep dependence on the amount of available KSPER current. The results establish that LRRC52 is a critical determinant of sperm KSPER function and essential to support normal fertility.

Author contributions: X.-H.Z., C.Y., X.-M.X., and C.J.L. designed research; X.-H.Z., C.Y., X.-M.X., and M.L. performed research; X.-M.X. contributed new reagents/analytic tools; X.-H.Z., C.Y., and C.J.L. analyzed data; and C.J.L. wrote the paper.

The authors declare no conflict of interest.

This article is a PNAS Direct Submission.

[1]To whom correspondence should be addressed. Email: clingle@morpheus.wustl.edu.

This article contains supporting information online at www.pnas.org/lookup/suppl/doi:10.1073/pnas.1423869112/-/DCSupplemental.

those of human KSPER (12). To evaluate the importance of the LRRC52 subunit, we have now generated *lrrc52*$^{-/-}$ (LRRC52 KO) mice. LRRC52 KO mice have a severe fertility deficit that is associated with a shift to more positive potentials in the KSPER current activation range in the LRRC52 KO sperm. Furthermore, measurement of the net KSPER current in sperm from two other genotypes, *slo3*$^{+/-}$ and a *slo3-eGFP,* suggests that sperm reproductive capacity strongly depends on the KSPER conductance available over physiological potentials. These results confirm that LRRC52 is a critical component of the KSPER channel complex and is essential for male fertility.

Results

***lrrc52*$^{-/-}$ Mice Have Severely Impaired Fertility.** Successful disruption of the *lrrc52* gene was confirmed by PCR (*Materials and Methods*). Western blots of membrane proteins of testis (Fig. S1*A*) or from WT and *lrrc52*$^{-/-}$ epididymal sperm confirmed that that LRRC52 protein was absent in LRRC52 KO mice (Fig. 1*A*). Consistent with previous observations (33), LRRC52 protein was also undetectable in epididymal sperm from *slo3*$^{-/-}$ mice (Fig. 1*A*). The absence of LRRC52 protein in *slo3*$^{-/-}$ sperm seems qualitatively similar to the loss of CatSper β (34) and δ (27) subunits in *CatSper*$^{-/-}$ sperm, suggesting that stability of auxiliary subunit protein requires assembly in a native channel complex.

A total of 17 *lrrc52*$^{-/-}$ males were each housed with two female WT mice for up to 100 d or until a litter was delivered. Of the 34 females, only eight litters were observed (Fig. 1*B*). In contrast, five *lrrc52*$^{+/-}$ males resulted in 10 litters from 10 females. The average number of days until birth following pairing of the males with the females was 24.9 ± 5.0 (mean ± SD) for the *lrrc52*$^{+/-}$ males and 63.1 ± 23.4 for the *lrrc52*$^{-/-}$ males (Fig. 1*C*). The average litter sizes were 5.7 ± 2.5 pups for the *lrrc52*$^{+/-}$ males and 1.6 ± 0.9 pups for the *lrrc52*$^{-/-}$ males (Fig. 1*D*). The mating results from *lrrc52*$^{+/-}$ males were similar to results with WT males. We conclude that LRRC52 is critical for mouse fertility, but the deficit is less than that observed for KO of the pore-forming SLO3 subunit (15, 21); no pups have been reported from mating of SLO3 KO males.

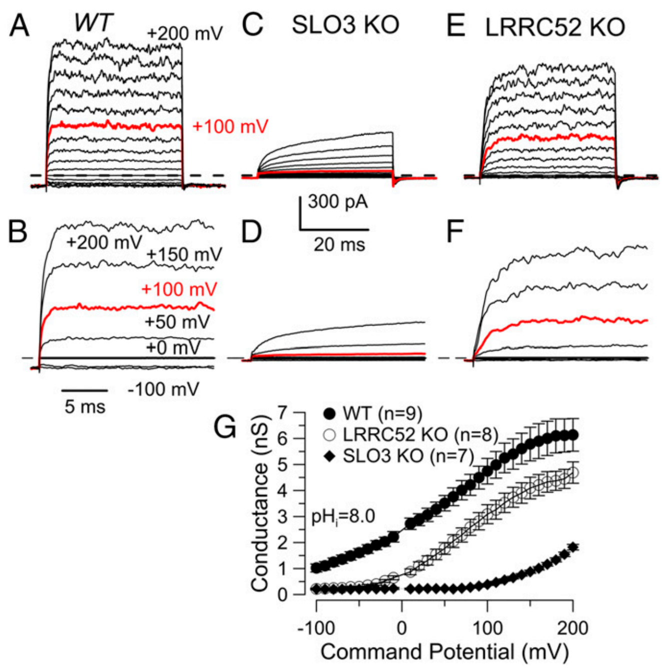

Fig. 2. KSPER current in corpus epididymal *lrrc52*$^{-/-}$ sperm is present but exhibits little activation at voltages negative to 0 mV. (*A*) Currents were activated at pipette pH 8.0 with voltage steps from −100 to +200 mV in a WT sperm. (*B*) Traces from *A* are shown at higher time resolution. (*C*) Currents were obtained under the same conditions as in *A* from a SLO3 KO sperm. (*D*) Traces from *C* are shown at higher time resolution. (*E*) Traces were from a LRRC52 KO sperm. (*F*) Traces from *E* are shown at higher time resolution. (*G*) Average (± SEM) conductance (measured from steady-state current levels) is plotted as a function of command potential for the three genotypes.

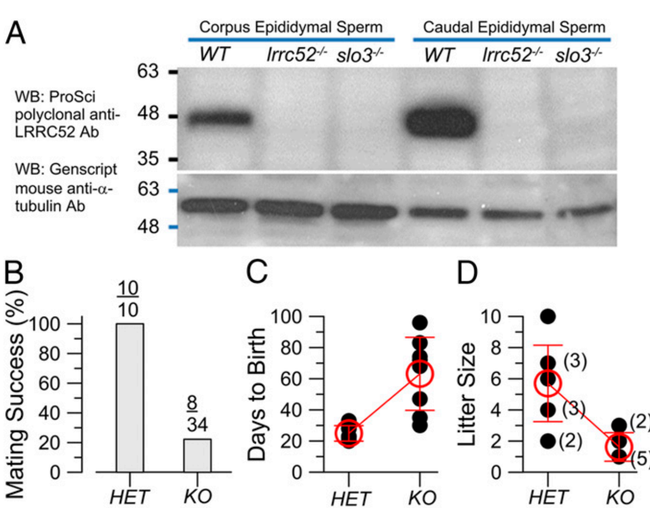

Fig. 1. Deletion of the LRRC52 subunit in mice results in severely impaired fertility. (*A*) Loss of LRRC52 protein following KO of the *lrrc52* gene was confirmed by Western blots. A ProSci polyclonal Ab recognizes a band of size consistent with LRRC52 in WT epididymal sperm proteins (corpus on left, cauda on right). The LRRC52 band is absent in *lrrc52*$^{-/-}$ and *slo3*$^{-/-}$ sperm. (*B*) Five *lrrc52*$^{+/-}$ and 17 *lrrc52*$^{-/-}$ KO males were each housed with two females and percent of females having litters is plotted (*lrrc52*$^{+/-}$: 10 of 10; *lrrc52*$^{-/-}$: 8/34). All females were naïve to mating. All $^{+/-}$ and $^{-/-}$ males in mating tests were obtained from matings of the same set of HET males with KO females. (*C*) The number of days until birth following pairing of males with females is shown. (*D*) The number of pups per litter is plotted for the various genotypes. Numbers in parentheses are the number of litters of a given size (e.g., there were five cases of only one pup per litter with KO males).

Corpus Epididymal Sperm from *lrrc52*$^{-/-}$ Mice Have KSPER Currents, but Activation Is Shifted to Positive Voltages. Whole-cell recordings were achieved using the sperm cytoplasmic droplet (10). The pipette solution was buffered to pH 8 to activate alkaline-dependent currents and a symmetrical 160 mM K^+ gradient was used. Currents were activated by 40-ms voltage steps from −100 to +200 mV in WT (Fig. 2 *A* and *B*), SLO3 KO (Fig. 2 *C* and *D*), and LRRC52 KO (Fig. 2 *E* and *F*) sperm. The raw current traces reveal several noteworthy features. First, both WT and LRRC52 KO currents show noticeably higher current variance than the SLO3 KO traces, consistent with the presence of an ion channel of large single-channel conductance in both the WT and LRRC52 KO sperm, but not in the SLO3 KO sperm. Second, over the range of 0 to +200 mV, the WT currents increase relatively linearly and the *slo3*$^{-/-}$ current only begins to show activation near +100 mV, whereas the *lrrc52*$^{-/-}$ current shows the beginning of weak current activation around 0 mV. GV curves generated from each of the genotypes indicates that KSPER current is markedly reduced at negative potentials in the LRRC52 KO sperm (Fig. 2*G*) relative to WT, although the maximum conductance at +200 mV only differs by about 25%. The residual current present in the *slo3*$^{-/-}$ sperm observed at potentials greater than about +80 mV reflects monovalent cation flux through CATSPER channels (19). As such, some of the conductance at positive potentials in both WT and LRRC52 KO sperm reflects the contributions of CATSPER. Despite uncertainty regarding the contributions of current through CATSPER channels, examination of the GV curves for WT and

LRRC52 KO sperm suggests that the voltages over which KSPER is activated at pH 8.0 are shifted rightward in the absence of LRRC52, with only small changes in maximal current amplitude. Notably, in the LRRC52 KO sperm, at pH 8.0 there is little conductance activated negative to 0 mV, whereas appreciable KSPER conductance is observed even at −100 mV in WT sperm.

Isolation of KSPER Current via KO of CATSPER Shows That the Primary Effect of LRRC52 KO Is to Shift Gating Rightward. To define the properties of isolated KSPER current in the presence and absence of LRRC52 without the contributions of CATSPER, we compared currents activated in CATSPER1 KO (Fig. 3 *A* and *B*) sperm to those in the double KO (dKO) of CATSPER1 and LRRC52 (Fig. 3 *C* and *D*). In both cases, the observed currents will reflect exclusively K^+ current through KSPER channels (19). The maximal peak conductances measured at +200 mV at pH 8 were 5.24 ± 0.2 nS for the CATSPER1 KO and 6.1 ± 0.7 nS for the CATSPER1/LRRC52 dKO. Despite the absence of CATSPER, the maximal conductance at positive potentials was generally similar to that observed in WT and LRRC52 KO sperm (Fig. 2). GV curves generated from the CATSPER KO sperm

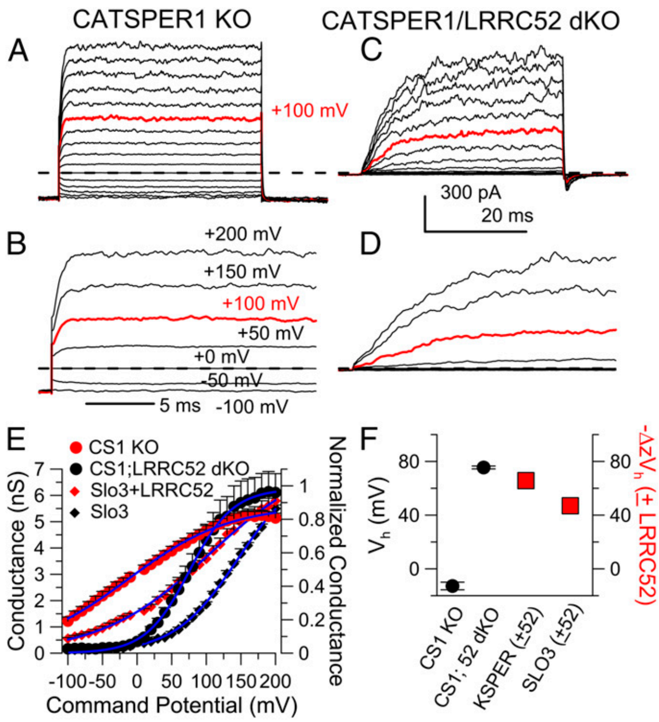

Fig. 3. KSPER gating shifts caused by LRRC52 KO are clearly defined in the absence of CATSPER. (*A*) Traces show isolated KSPER current from a CATSPER1 KO sperm at pH_i 8.0. (*B*) Traces show currents from *A* at faster time resolution. (*C*) Traces show isolated KSPER current from a sperm lacking both CATSPER1 and LRRC52 at pH_i 8.0. (*D*) Traces are currents from *C* at a faster time base. (*E*) GV curves were generated for both CATSPER1 KO sperm (eight cells) and for LRRC52/CATSPER1 double KO sperm (seven cells). Boltzmann fit to dKO GV yielded $G_{max} = 6.3 \pm 0.1$ nS, with $V_h = 75.5 \pm 1.1$ mV and $z = 0.8e \pm 0.02$. Fit to CATSPER1 KO yielded $G_{max} = 5.6 \pm 0.1$ nS with $V_h = -12.8 + 2.8$ mV with $z = 0.35e \pm 0.01$. Errors are 95% confidence limits on the fitted parameter. Normalized GV curves (pH 8.0, normalized to conductance measured at +250 mV) from expression of SLO3 and SLO3+LRRC52 in oocytes are also shown along with Boltzmann fits (SLO3: V_h = 145.6 ±1.8; $z = 0.56 \pm 0.01e$; SLO3+LRRC52: $V_h = 104.4 \pm 4.0$ mV, $z = 0.33 \pm 0.01e$). Data from ref. 33. (*F*) Left axis plots average V_h for KSPER currents from CATSPER1 KO and CATSPER1/LRRC52 dKO sperm. Right axis plots the change in zV_h for KSPER current with and without LRRC52 (in the CATSPER1 KO background) along with the zV_h for heterologously expressed SLO3 current with and without LRRC52.

(Fig. 3*E*) allowed comparison of the maximal conductance and voltages of half activation (V_h) for KSPER in the presence and absence of LRRC52. Both GV curves suggest that at positive potentials with pipette pH 8.0, saturation in activation of KSPER conductance is achieved, therefore allowing estimates of the V_h for KSPER current with and without LRRC52 (Fig. 3*F*). In the CATSPER KO background, at pipette pH 8.0, the V_h of KSPER conductance arising from SLO3 channels containing LRRC52 subunits is about −12.8 ± 2.8 mV, whereas in the absence of LRRC52 the V_h shifts about 85 mV to 75.5 ± 1.1 mV. Normalized GVs from previous work (33) that compared currents in oocytes resulting from expression of SLO3 alone and SLO3+LRRC52 are also shown over a similar voltage range (Fig. 3*E*) The V_h values for the KSPER currents with or without LRRC52 differ from those measured in *Xenopus* oocytes, with or without LRRC52 (33). However, V_h alone is not an accurate indicator of the energetic consequences of the impact of LRRC52. To provide a better assessment of the impact of LRRC52 expression both in sperm and in oocytes, we calculated the change in free energy of the channel gating equilibrium, $-\Delta zV_h$, that arises from the presence of LRRC52 (35), where $\Delta zV_h = zV_{h(+LRRC52)} - zV_{h(-LRRC52)}$ for KSPER or SLO3 currents with or without LRRC52 (Fig. 3*F*, right). The magnitude of the LRRC52-induced shift in $-\Delta zV_h$ in mouse sperm is quite similar to that determined for the LRRC52-induced shift for mSLO3 currents expressed heterologously (33). It should be kept in mind that the estimation of $-\Delta zV_h$ is also not without limitations, particularly given that the GVs are not truly Boltzmann, but reflect a complicated set of coupled allosteric equilibria (30, 36). Despite these cautionary remarks, the present results demonstrate that the primary consequence of LRRC52 deletion is a rightward shift in the range of activation of KSPER current at a given pH, which is true both in sperm and in heterologous expression of SLO3. These results indicate that the LRRC52 subunit is an essential component of the KSPER channel complex and critically define the range of voltages over which KSPER current activates at a given pH. That the exact V_h values differ between mSLO3 and KSPER in sperm may indicate that other components of KSPER channels remain to be identified.

KSPER Conductance Is Reduced in Sperm from *slo3*$^{+/-}$ and *slo3-eGFP* Mice. That mating of WT females with LRRC52 KO males yielded some live pups prompted us to wonder how much residual KSPER current is required to support at least some fertility, no matter how compromised. We previously observed that KSPER current activated by voltage ramps to +100 mV in sperm from *slo3*$^{+/-}$ mice (SLO3 HET) was about half that observed in WT sperm (15). Furthermore, to generate the SLO3 KO mouse, we had introduced an eGFP ORF into the Cre-LoxP bracketed target exon. Such mice seemed to breed normally, but we noted that the total KSPER current in the *slo3-eGFP* sperm was reduced even further in comparison with the *slo3*$^{+/-}$ sperm (15). Given the altered fertility in the LRRC52 KO mice, one might therefore wonder why fertility difficulties in the *slo3-eGFP* mice were not previously observed. We have therefore examined the relationship between the KSPER current and fertilization capacity in the *slo3*$^{+/-}$ and *slo3-eGFP* genotypes.

KSPER currents were activated by voltage steps up to +200 mV with pipette pH 8 in *slo3*$^{+/-}$ sperm (Fig. 4 *A* and *B*). Peak conductance at +200 mV was reduced to less than half of that in WT sperm. Considering that CATSPER also contributes a portion of the monovalent flux measured at +200 mV in both WT and *slo3*$^{+/-}$ sperm, the reduction of current in *slo3*$^{+/-}$ sperm may be even greater. The *slo3-eGFP* sperm exhibited a similar reduction in maximum KSPER current (Fig. 4 *C* and *D*) in comparison with WT sperm. Comparison of GV curves from WT, *slo3*$^{+/-}$, *slo3-eGFP*, and LRRC52 KO sperm (Fig. 4*E*) shows that maximum KSPER current is substantially larger in the LRRC52

PHYSIOLOGY

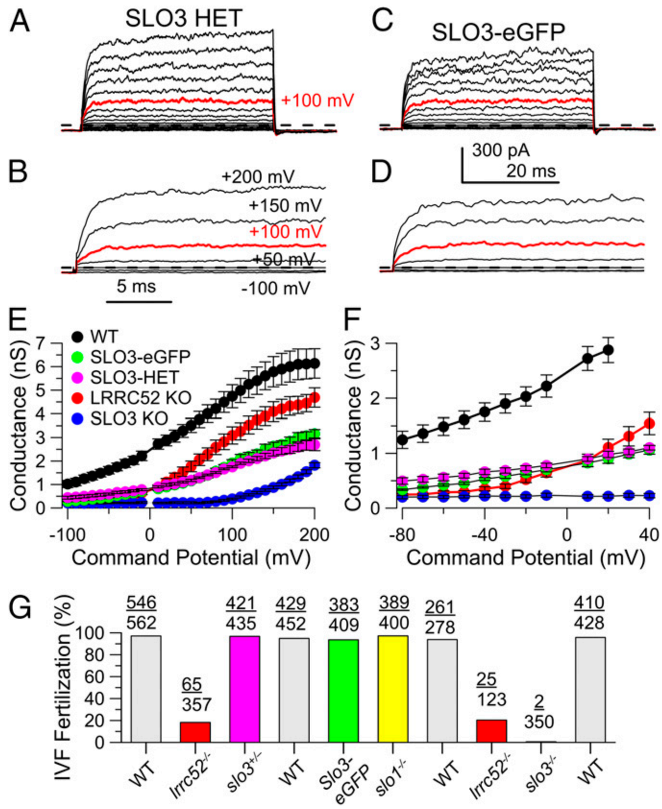

Fig. 4. KSPER current is reduced in both *slo3*$^{+/-}$ and *slo3-eGFP* sperm. (*A*) Traces show current from a *slo3*$^{+/-}$ sperm (SLO3 HET) at pH_i 8.0. (*B*) Traces show currents from *A* at faster time resolution. (*C*) Traces show isolated KSPER current from a sperm expressing the *slo3-eGFP* allele at pH_i 8.0. (*D*) Traces are currents from *C* at a faster time base. Calibration bars in *B* apply to both *A* and *B*. (*E*) GV curves are plotted for WT, SLO3-eGFP, SLO3 HET, LRRC52 KO, and SLO3 KO. (*F*) GV curves from the indicated genotypes in *E* are shown for voltages up to +40 mV to highlight differences over a physiological range of potentials. (*G*) Percent of two-cell embryos observed in IVF assays are shown for various genotypes. Numbers at the top reflect number of two-cell embryos over the total number of embryos examined. IVF results are presented in their temporal order over a several-month period.

KO sperm than in either the SLO3 heterozygotes or the SLO3-eGFP sperm. However, inspection of the GV curves at more negative potentials (Fig. 4*F*) shows that more KSPER is activated in both the *slo3*$^{+/-}$ and *slo3-eGFP* sperm than in LRRC52 KO sperm at membrane potentials between −10 and −60 mV. This difference arises because of the rightward gating shift of the KSPER current in the LRRC52 KO sperm, in comparison with *slo3*$^{+/-}$ and *slo3-eGFP* sperm, presumably reflecting the absence or presence of the LRRC52 subunits. We, in fact, confirmed that LRRC52 was present in *slo3*$^{-/-}$ and *slo3-eGFP* testis (Fig. S1).

Given the reduced KSPER current in the *slo3-eGFP* sperm, we reexamined mating properties of *slo3-eGFP* mice. A set of five *slo3-eGFP* males resulted in successful litters in 10 females. The average time to birth following pairing of male and female mice was 24.9 ± 5.0 d and the average litter size was 5.7 ± 2.5, both values similar to those obtained with WT males mated to naïve females. We also performed an in vitro fertilization (IVF) assay (Fig. 4*G*) on the various genotypes examined here (Fig. 4*G*) as a measure of the reproductive competence of these sperm. This included WT, *lrrc52*$^{-/-}$, *slo3*$^{-/-}$, *slo3*$^{+/-}$, and *slo3-eGFP*. Because of some results suggesting that the Ca^{2+}- and voltage-activated BK-type current may also play a role in at least some mammalian sperm (11, 37), we also included *slo1*$^{-/-}$ sperm in our IVF tests. IVF success was markedly suppressed in *lrrc52*$^{-/-}$ sperm, although not as much as in *slo3*$^{-/-}$ sperm. In contrast, IVF success was indistinguishable among WT, *slo3*$^{+/-}$, *slo3-eGFP*, and *slo1*$^{-/-}$ sperm. That apparently normal fertilization capability persists in the *slo3*$^{+/-}$ and *slo3-eGFP* sperm, despite the substantial decrease in total amount of KSPER available to be activated, shows that marked decrements in KSPER can occur without any detectable changes in IVF fertilization capability. Furthermore, at least in mice, a complete absence of BK/SLO1 channels produces no change in IVF capability.

Alkaline pH Is Less Effective at Producing Hyperpolarization in *lrrc52*$^{-/-}$ Sperm Compared with WT Sperm or Other Genotypes. At low pH, mouse sperm membrane potential is considered to be in the range of −20 to 0 mV (14, 15), whereas alkalization, by eliciting activation of KSPER, drives membrane potentials (V_m) more negative. In WT sperm, a membrane potential of about −40 mV is reached as pH is elevated to between pH 7 and 8. It is therefore important to determine to what extent the changes in net KSPER conductance may affect the ability of alkalization to drive V_m changes. Previous work demonstrated that the decrease in net KSPER current in *slo3*$^{+/-}$ sperm had no obvious effect on fertility and only mildly altered the pH-dependent change in V_m (15). Given that KSPER current is present in *lrrc52*$^{-/-}$ sperm and that some successful matings were achieved with *lrrc52*$^{-/-}$ mice, we therefore compared the ability of pipette pH_i of 6, 7, or 8 to define V_m for *WT*, *slo3*$^{-/-}$, *lrrc52*$^{-/-}$, *slo3-eGFP*, and *slo3*$^{+/-}$ sperm (Fig. 5*A*). Compared with pH 6, pH 7 resulted in an over −20-mV hyperpolarization in *WT* and *slo3*$^{+/-}$ sperm, and a somewhat weaker hyperpolarization in *slo3-eGFP* sperm, with an additional −10- to −20-mV change at pH 8.0. In contrast, the change from pH 6–7 produced no significant membrane hyperpolarization in either *slo3*$^{-/-}$ or *lrrc52*$^{-/-}$ sperm. Additional alkalization from 7 to 8 was able to produce hyperpolarization in *lrrc52*$^{-/-}$ sperm, but not in *slo3*$^{-/-}$ sperm. Although at pH 8 the V_m measurements did not differ between *lrrc52*$^{-/-}$ sperm and *slo3-eGFP* sperm (P = 0.18), the V_m measurements at pH 7 differed ($P < 0.001$).

The relative ability of pipette alkalization to produce hyperpolarization among sperm of different genotypes correlates generally with the relative amounts of KSPER activated at pH 8.0 at negative potentials among those genotypes (Fig. 4*F*), rather than the maximal KSPER able to be activated in a given genotype. Intriguingly, differences in V_m among sperm in response to alkalization are more apparent at pH 7, whereas with pipette pH 8 the differences are weaker or absent. Although our results do not provide an explanation for why differences in V_m at pH 8 are smaller among genotypes than at pH 7, it should be noted that V_m will not vary linearly with the amount of KSPER activation. In fact, despite an over twofold increase in KSPER current activation in mouse sperm with an increase in pipette pH from 7 to 8, only modest additional hyperpolarization occurs in WT sperm with changes in pipette pH from 7 to 8 (14). It should also be remembered that alkalization will also activate CATSPER, which will favor depolarization of V_m, probably accounting for the V_m positive to 0 mV observed at pH 8 in SLO3 KO sperm.

At pH 6, mouse sperm V_m measured by patch clamp is in the range of −15 to 0 mV, as observed here and previously (14, 15). Alkalization that elicits KSPER activation drives V_m to values as negative as around −40 to −50 mV (14, 15). The availability of KSPER for activation at potentials just negative to 0 mV should therefore be the primary determinant of the effectiveness of KSPER in supporting normal sperm function and fertility. As one measure of the dependence of fertilization competence on KSPER, we therefore plotted the IVF success (Fig. 5*C*) and pups per pairing (Fig. 5*D*) for different genotypes as a function of the mean KSPER conductance that was observed at −40 mV with pipette pH 8 (G_{KSPER} at −40 mV). A membrane potential of −40 mV seems a reasonable approximation of that which may be occurring in response to alkalization within the female reproductive tract. The

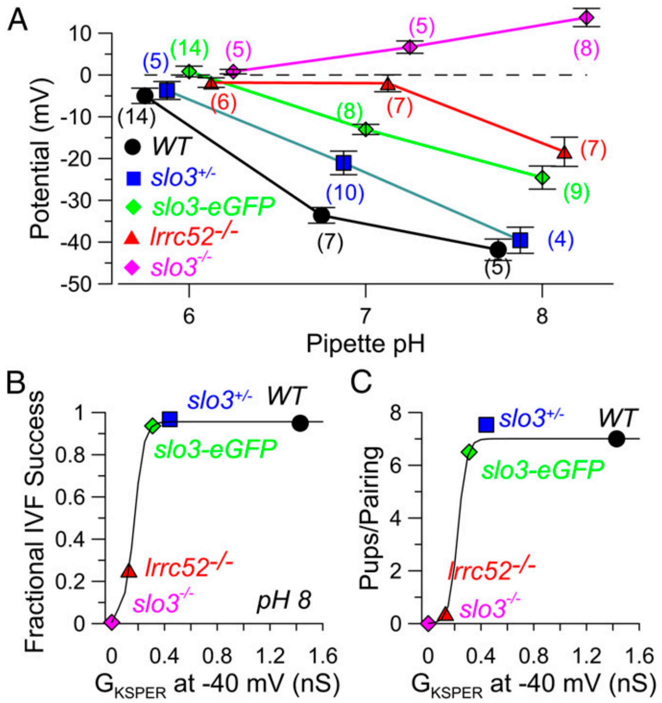

Fig. 5. Alkalization is less effective at producing hyperpolarization in lrrc52 KO sperm. (*A*) Membrane potential measurements were made from sperm of the indicated genotypes at various pipette pH. Symbols and error bars correspond to mean ± SEM. Numbers in parentheses indicate number of tested sperm for a given condition. Points are offset from the nominal pH for visual clarity. At pH 7, WT differs from *slo3*$^{+/-}$ at $P < 0.005$, and, for all other genotypes, at $P < 0.001$. At pH 8, WT differs from *lrrc52*$^{-/-}$ and *slo3-eGFP* differ at $P < 0.001$ and $P < 0.002$, respectively. At pH 7, *lrrc52*$^{-/-}$ differs from *slo3-eGFP* and *slo3*$^{+/-}$ at $P < 0.001$. At pH 8, *lrrc52*$^{-/-}$ and *slo3-eGFP* differ at $P < 0.01$. (*B*) Fractional IVF success was plotted as a function of the net conductance, G_{KSPER}, measured at −40 mV. Net G_{KSPER} was the difference between the measured conductance for a given genotype, minus the mean conductance measured at −40 mV for the *slo3*$^{-/-}$ sperm. Solid lines in *B* and *C* are without mechanistic significance. (*C*) The average number of pups per male–female pairing (including pairings yielding no pups) is plotted as a function of G_{KSPER}.

resulting relationships between G_{KSPER} and IVF success and mating success are consistent with the idea that reproductive competence exhibits a steep dependence on the absolute amount of KSPER conductance that can be activated at pH 8 in a given genotype.

Discussion

The present results establish that the LRRC52 protein is essential for normal male fertility and is a key element, along with SLO3, in defining the functional properties of the KSPER channel complex. LRRC52 must now be included in the number of proteins, most of which are sperm-specific, that are associated with ion transport functions and that have been established to play critical roles in supporting male fertility. This includes CATSPER α (1–4, 13, 23, 25, 38) and CATSPER δ (27) subunits, SLO3 (15, 21), the NHE5 Na^+–H^+ exchanger (39), and the Na,K-ATPase α4 isoform (40). The one protein so far identified that is involved in sperm ion flux and seems critical for fertility, but is not sperm-specific, is the PMCA4 Ca-ATPase (41, 42).

An intriguing aspect of the present observations is that, unlike SLO3 KO, which produces complete absence of fertility, the LRRC52 KO males exhibited a severe, but incomplete, loss of fertility. Given the changes that LRRC52 KO produces in KSPER, one wonders why any fertilization occurs at all. Even at pH_i 8, KSPER in LRRC52 KO sperm is only weakly activated at voltages negative to 0 in comparison with WT. This is compatible with current-clamp results indicating that, even at pH_i 7, there is insufficient activation of KSPER current in LRRC52 KO sperm to mediate hyperpolarization. Only at pH 8 is hyperpolarization observed. Together, the results imply that the loss of fertility specifically results from inability of KSPER in the LRRC52 KO sperm to mediate the required changes in V_m in response to alkalization. That LRRC52 KO sperm are less severely compromised than SLO3 KO sperm suggests that even a small net KSPER conductance over voltages from −10 to −40 mV may be sufficient to support some fertilization competence.

Comparison of our results from sperm of different genotypes, including *slo3*$^{+/-}$ and *slo3-eGFP* sperm, implies a steep dependence of fertility on available KSPER conductance. Both *slo3*$^{+/-}$ and *slo3-eGFP* sperm show reduced levels of maximal KSPER conductance relative to LRRC52 KO but show relatively normal fertility. This apparently arises because, despite the reduction in maximal KSPER, for both *slo3*$^{+/-}$ and *slo3-eGFP* sperm activation of KSPER over potentials from −40 to −10 mV is larger than for the LRRC52 KO sperm. We therefore propose that the critical factor in the ability of KSPER to support effective fertility is the extent to which KSPER can be activated over physiological potentials (e.g., −10 to −40 mV). Thus, despite the larger maximal KSPER conductance in LRRC52 KO sperm compared with the SLO3-eGFP sperm, the shifted KSPER gating in LRRC52 KO sperm results in an amount of KSPER conductance at physiological potentials that is apparently insufficient to support normal fertility.

In WT sperm, a membrane potential of about −40 mV is reached between pH 7 and 8 (14, 15). The KSPER conductance that is activated at −40 mV at pH 8 might therefore be considered a rough approximation of the amount of KSPER that might be maximally activated during physiologically induced alkalization. We therefore plotted the IVF success (Fig. 5*C*) and pups per pairing (Fig. 5*D*) for different genotypes as a function of the mean KSPER conductance able to be activated at −40 mV with pipette pH 8. Although there are many intervening steps between alkalization and fertilization, these panels suggest that reproductive competence exhibits a steep dependence on the absolute amount of KSPER conductance that can be activated at pH 8 at a physiologically important potential (−40 mV) in a given genotype.

The present results suggest that even a small amount of K^+ current activation may be sufficient to support the sperm functions necessary for fertilization. Assuming that the average amount of KSPER we observe in noncapacitated sperm of different genotypes is maintained through all stages of sperm maturation up until fertilization, this implies that mouse sperm apparently have a very large safety factor in terms of the KSPER current required to support normal fertilization. If so, this therefore raises some question regarding KSPER as a potential target for male contraceptives. For mice, perhaps more than 90% of the KSPER current normally activated during alkalization would need to be inhibited to produce complete inhibition of fertility. Development of a compound that produces 90% or greater inhibition of KSPER without affecting other targets may be challenging. However, given the differences in fecundity between mice and humans, such considerations may not be entirely applicable to human reproduction. Another possibility is that perhaps KSPER current density at later stages of sperm maturation may be larger than observed in the noncapacitated sperm examined here. If so, the fertilization competence of the genotypes examined here might reflect KSPER current densities at later developmental times. At present, we know of no information that clearly addresses this issue.

LRRC52 protein is also present in human sperm (12, 43), and human LRRC52 coassembles with human SLO3 to produce channels that are regulated in a fashion similar to native human KSPER current (12). An interesting aspect of human SLO3 is that, in contrast to mouse SLO3, it is activated by increases in cytosolic Ca^{2+} (12) and more weakly by alkalization (12, 44). The

PHYSIOLOGY

differential regulation of mSLO3 and hSLO3 is not surprising given the relatively low ~70% homology in their ligand-sensing cytosolic domains. That human KSPER is Ca^{2+}-activated has also resulted in the proposals that the Ca^{2+}-activated SLO1 K^+ channel is present in human sperm (11) and that both SLO1 and SLO3 may be present (37). As yet, SLO1 protein has not been detected in human sperm. Given that cases of infertile CATSPER-deficient humans have been identified (18, 45), the discovery of human KSPER-deficient males might help resolve this issue and perhaps also reveal examples of infertility arising from deficits in human LRRC52.

The marked dependence of mouse sperm function and fertility on KSPER raises several questions. Are the unique properties of mouse KSPER, that is, its pH dependence, mild voltage dependence, and relatively low operational open probabilities, specifically tailored for its role in mouse sperm physiology? Given the rapid evolution of sperm-specific proteins and the changes in regulation of such proteins among species, are such changes associated with unique species-specific differences in sperm function that depend on the unique properties of their ion channels? Given the paucity of other K^+ conductances in the SLO3 KO sperm, reintroduction into sperm of SLO3 KO mice of alternative K^+ genes under sperm-specific promoter control might provide some insight into the specific requirements for mSLO3 in mouse sperm function.

Materials and Methods

Generation of *lrrc52*$^{-/-}$ Mice and *CatSper1*$^{-/-}$/*lrrc52*$^{-/-}$ dKO Mice. Details of generation of the *lrrc52*$^{-/-}$ mice and the dKO with CatSper1 are provided in *SI Materials and Methods*.

Animal Husbandry and Procedures. All animal husbandry and experimental procedures were approved by and performed in accordance with guidelines of the Washington University School of Medicine Animal Care and Use Committee.

Electrophysiology. Sperm recordings were done on noncapacitated sperm followed methods previously used in this laboratory (15, 33). Additional details are given in *SI Materials and Methods*.

Protein Preparation, Immunoprecipitation, and Western Blotting. Sperm total proteins of mouse corpus and cauda epididymis and testis membrane proteins were prepared using previously described protocols (15, 33). Additional details are given in *SI Materials and Methods*.

IVF. IVF tests were performed by Harry Fraser of the Mouse Genetics Core at Washington University School of Medicine. Additional details are provided in *SI Materials and Methods*.

ACKNOWLEDGMENTS. We thank Harry Fraser for performing the in vitro fertilization assays. This work was supported by NIH Grant GM-081748 (to C.J.L.) and Natural Science Foundation of China Grants 31230034 and 31171116 (to X.-H.Z.).

1. Yanagimachi R (1969) In vitro capacitation of hamster spermatozoa by follicular fluid. *J Reprod Fertil* 18(2):275–286.
2. Suarez SS (1996) Hyperactivated motility in sperm. *J Androl* 17(4):331–335.
3. Ho HC, Suarez SS (2001) Hyperactivation of mammalian spermatozoa: Function and regulation. *Reproduction* 122(4):519–526.
4. Suarez SS (2008) Control of hyperactivation in sperm. *Hum Reprod Update* 14(6): 647–657.
5. Babcock DF, Pfeiffer DR (1987) Independent elevation of cytosolic [Ca^{2+}] and pH of mammalian sperm by voltage-dependent and pH-sensitive mechanisms. *J Biol Chem* 262(31):15041–15047.
6. Wennemuth G, Carlson AE, Harper AJ, Babcock DF (2003) Bicarbonate actions on flagellar and Ca^{2+} -channel responses: Initial events in sperm activation. *Development* 130(7):1317–1326.
7. Darszon A, et al. (2005) Calcium channels and Ca^{2+} fluctuations in sperm physiology. *Int Rev Cytol* 243:79–172.
8. Kirichok Y, Navarro B, Clapham DE (2006) Whole-cell patch-clamp measurements of spermatozoa reveal an alkaline-activated Ca^{2+} channel. *Nature* 439(7077):737–740.
9. Navarro B, Kirichok Y, Chung JJ, Clapham DE (2008) Ion channels that control fertility in mammalian spermatozoa. *Int J Dev Biol* 52(5–6):607–613.
10. Kirichok Y, Lishko PV (2011) Rediscovering sperm ion channels with the patch-clamp technique. *Mol Hum Reprod* 17(8):478–499.
11. Mannowetz N, Naidoo NM, Choo SA, Smith JF, Lishko PV (2013) Slo1 is the principal potassium channel of human spermatozoa. *eLife* 2:e01009.
12. Brenker C, et al. (2014) The Ca^{2+}-activated K^+ current of human sperm is mediated by Slo3. *eLife* 3:e01438.
13. Ren D, et al. (2001) A sperm ion channel required for sperm motility and male fertility. *Nature* 413(6856):603–609.
14. Navarro B, Kirichok Y, Clapham DE (2007) KSper, a pH-sensitive K^+ current that controls sperm membrane potential. *Proc Natl Acad Sci USA* 104(18):7688–7692.
15. Zeng XH, Yang C, Kim ST, Lingle CJ, Xia XM (2011) Deletion of the Slo3 gene abolishes alkalization-activated K^+ current in mouse spermatozoa. *Proc Natl Acad Sci USA* 108(14):5879–5884.
16. Lishko PV, Botchkina IL, Fedorenko A, Kirichok Y (2010) Acid extrusion from human spermatozoa is mediated by flagellar voltage-gated proton channel. *Cell* 140(3): 327–337.
17. Lishko PV, Botchkina IL, Kirichok Y (2011) Progesterone activates the principal Ca^{2+} channel of human sperm. *Nature* 471(7338):387–391.
18. Smith JF, et al. (2013) Disruption of the principal, progesterone-activated sperm Ca2+ channel in a CatSper2-deficient infertile patient. *Proc Natl Acad Sci USA* 110(17): 6823–6828.
19. Zeng XH, Navarro B, Xia XM, Clapham DE, Lingle CJ (2013) Simultaneous knockout of Slo3 and CatSper1 abolishes all alkalization- and voltage-activated current in mouse spermatozoa. *J Gen Physiol* 142(3):305–313.
20. Chávez JC, et al. (2014) SLO3 K^+ channels control calcium entry through CATSPER channels in sperm. *J Biol Chem* 289(46):32266–32275.
21. Santi CM, et al. (2010) The SLO3 sperm-specific potassium channel plays a vital role in male fertility. *FEBS Lett* 584(5):1041–1046.
22. Carlson AE, et al. (2003) CatSper1 required for evoked Ca^{2+} entry and control of flagellar function in sperm. *Proc Natl Acad Sci USA* 100(25):14864–14868.
23. Quill TA, et al. (2003) Hyperactivated sperm motility driven by CatSper2 is required for fertilization. *Proc Natl Acad Sci USA* 100(25):14869–14874.
24. Carlson AE, et al. (2005) Identical phenotypes of CatSper1 and CatSper2 null sperm. *J Biol Chem* 280(37):32238–32244.
25. Jin J, et al. (2007) Catsper3 and Catsper4 are essential for sperm hyperactivated motility and male fertility in the mouse. *Biol Reprod* 77(1):37–44.
26. Qi H, et al. (2007) All four CatSper ion channel proteins are required for male fertility and sperm cell hyperactivated motility. *Proc Natl Acad Sci USA* 104(4):1219–1223.
27. Chung JJ, Navarro B, Krapivinsky G, Krapivinsky L, Clapham DE (2011) A novel gene required for male fertility and functional CATSPER channel formation in spermatozoa. *Nat Commun* 2:153.
28. Schreiber M, et al. (1998) Slo3, a novel pH-sensitive K^+ channel from mammalian spermatocytes. *J Biol Chem* 273(6):3509–3516.
29. Butler A, Tsunoda S, McCobb DP, Wei A, Salkoff L (1993) mSlo, a complex mouse gene encoding "maxi" calcium-activated potassium channels. *Science* 261(5118):221–224.
30. Zhang X, Zeng X, Lingle CJ (2006) Slo3 K^+ channels: Voltage and pH dependence of macroscopic currents. *J Gen Physiol* 128(3):317–336.
31. Zhang X, Zeng X, Xia X-M, Lingle CJ (2006) pH-regulated Slo3 K^+ channels: properties of unitary currents. *J Gen Physiol* 128(3):301–315.
32. Yan J, Aldrich RW (2010) LRRC26 auxiliary protein allows BK channel activation at resting voltage without calcium. *Nature* 466(7305):513–516.
33. Yang C, Zeng XH, Zhou Y, Xia XM, Lingle CJ (2011) LRRC52 (leucine-rich-repeat-containing protein 52), a testis-specific auxiliary subunit of the alkalization-activated Slo3 channel. *Proc Natl Acad Sci USA* 108(48):19419–19424.
34. Liu J, Xia J, Cho KH, Clapham DE, Ren D (2007) CatSperbeta, a novel transmembrane protein in the CatSper channel complex. *J Biol Chem* 282(26):18945–18952.
35. Cui J, Aldrich RW (2000) Allosteric linkage between voltage and Ca($^{2+}$)-dependent activation of BK-type mslo1 K($^+$) channels. *Biochemistry* 39(50):15612–15619.
36. Horrigan FT, Aldrich RW (2002) Coupling between voltage sensor activation, Ca^{2+} binding and channel opening in large conductance (BK) potassium channels. *J Gen Physiol* 120(3):267–305.
37. López-González I, et al. (2014) Membrane hyperpolarization during human sperm capacitation. *Mol Hum Reprod* 20(7):619–629.
38. Quill TA, Ren D, Clapham DE, Garbers DL (2001) A voltage-gated ion channel expressed specifically in spermatozoa. *Proc Natl Acad Sci USA* 98(22):12527–12531.
39. Wang D, King SM, Quill TA, Doolittle LK, Garbers DL (2003) A new sperm-specific Na^+/H^+ exchanger required for sperm motility and fertility. *Nat Cell Biol* 5(12):1117–1122.
40. Jimenez T, McDermott JP, Sánchez G, Blanco G (2011) Na,K-ATPase alpha4 isoform is essential for sperm fertility. *Proc Natl Acad Sci USA* 108(2):644–649.
41. Okunade GW, et al. (2004) Targeted ablation of plasma membrane Ca^{2+}-ATPase (PMCA) 1 and 4 indicates a major housekeeping function for PMCA1 and a critical role in hyperactivated sperm motility and male fertility for PMCA4. *J Biol Chem* 279(32): 33742–33750.
42. Schuh K, et al. (2004) Plasma membrane Ca^{2+} ATPase 4 is required for sperm motility and male fertility. *J Biol Chem* 279(27):28220–28226.
43. Wang G, et al. (2013) In-depth proteomic analysis of the human sperm reveals complex protein compositions. *J Proteomics* 79:114–122.
44. Leonetti MD, Yuan P, Hsiung Y, Mackinnon R (2012) Functional and structural analysis of the human SLO3 pH- and voltage-gated K^+ channel. *Proc Natl Acad Sci USA* 109(47):19274–19279.
45. Hildebrand MS, et al. (2010) Genetic male infertility and mutation of CATSPER ion channels. *Eur J Hum Genet* 18(11):1178–1184.